

Evolution of turbulent heat flux across a shock wave

Russell Quadros, Palash Sashittal, Ashwin Ramachandran and Krishnendu Sinha

Department of Aerospace Engineering, Indian Institute of Technology Bombay, Mumbai 400076, India

Abstract

Turbulent heat flux vector $\overline{u'_j T'}$ is an unclosed term in the Reynolds Averaged energy conservation equation. Accurate modeling of this term in shock-dominated flows is important for accurate prediction of wall heat transfer rate. We study the generation of turbulent heat flux vector $\overline{u'_j T'}$ in a canonical interaction of homogeneous isotropic turbulence with a normal shock wave. The upstream turbulence considered is purely vortical in nature. The total enthalpy conservation equation across the unsteady shock wave is written in a linearized form and is used to develop a transport equation for $\overline{u'_j T'}$. A budget for the source terms integrated across the time-averaged shock wave is calculated using Linear Interaction Analysis, both for 2D component waves and a 3D isotropic spectrum. We thus identify the dominant mechanisms responsible for the generation of $\overline{u'_j T'}$ across the shock. The validity of Morkovin's hypothesis is also discussed.

1. Introduction

A commonly observed phenomenon in high speed flows is interaction of turbulent boundary layer with shock wave. It occurs in configurations such as intakes of air-breathing engines, rocket nozzles, flow over transonic airfoils and wing body junctions of high speed vehicles. The region where such an interaction occurs is marked with drastic increase in wall pressure and wall heat flux. These may further be accompanied by additional flow features such as separation bubble and multiple shock/expansion waves. Accuracy in computational prediction of such phenomenon is important for design of aerospace vehicles.

Engineering simulations of high speed turbulent flows rely largely on Reynolds averaged Navier-Stokes (RANS) methodology. The RANS equations, obtained by averaging the full Navier-Stokes equations, solve for the mean flow quantities. The unclosed terms present in these averaged equations represent the effect of turbulence on the mean flow and are modeled in terms of mean flow quantities and closure coefficients. Accurate predictions of shock-based flows using conventional RANS turbulence models is a challenging task. Conventional models often fail to capture essential flow features such as separation bubble size and peak wall pressure/heat flux.

Several researchers have suggested modeling improvements for cases involving shock-turbulence interaction. At the region of shock, gradient diffusion based Reynolds stress models yield unrealistically high values. Thivet et al. [1], Durbin [2] and Shih et al. [3] proposed modification to this hypothesis by restricting the value of eddy viscosity. This restrains the magnitude of Reynolds stress, which in-turn reduces the production of TKE. These corrections have led to improved prediction of TKE amplification but are still high on comparison to DNS data [4]. Sinha et al. [4] propose an additional correction to include the effect of unsteady shock motion in shock-turbulence interaction, and the shock-unsteadiness model matches DNS data well. Application of this model to cases of shock-boundary layer interaction problems yields improved prediction of separation bubble size and pressure data [5], [6], [7]. In spite of these improvements, surface heat flux is inaccurately predicted by most turbulence models.

An unclosed term in energy conservation equation is $\overline{u'_j T'}$ which is known as turbulent heat flux vector. Here u'_j denotes the velocity fluctuation in the j^{th} direction and T' denotes the temperature fluctuation. The overline represents time averaging. This term has significant values in boundary layer and influences the distribution of mean temperature, which in-turn determines the wall heat flux. The value of $\overline{u'_j T'}$ upstream of the shock also has significant effect on TKE amplification which determines flow features such as the separation bubble size and surface pressure distribution.

Modeling of turbulent heat flux in conventional RANS models is based on Strong Reynolds Analogy proposed by Morkovin [8]. It is based on the fact that the momentum and energy conservation equations take analogous form in zero pressure gradient boundary layers at high Reynolds number. Further, the total temperature fluctuations are negligible in the absence of wall heat transfer. This allows a relation between the streamwise velocity and temperature fluctuations given by

$$\frac{T'_{rms}}{\bar{T}} = (\gamma - 1)M^2 \frac{u'_{rms}}{\bar{u}} \quad (1)$$

where bar represents the mean flow values and γ denotes the ratio of specific heats. The above equation can be translated to give the following expression for the correlation coefficient, R_{uT} between velocity and temperature fluctuations

$$R_{uT} = \frac{\overline{u'T'}}{u'_{rms}T'_{rms}} = -1$$

Turbulent Prandtl number, Pr_T used in modeling turbulent heat flux takes a value of 1 based on the above assumptions. In practise, a constant value of $Pr_T = 0.89$ is used in turbulent boundary layers.

Mahesh et al. [9] investigated the validity of Morkovin's hypothesis across a shock wave using Linear Interaction Analysis and DNS. They studied the case of homogeneous isotropic turbulence passing through a normal shock. The upstream turbulence with vortical and entropy fluctuations was chosen so as to satisfy Morkovin's hypothesis i.e. $R_{uT} = -1$. Total temperature fluctuations were found to be non-negligible behind the shock. Eq. (1) which relies on this assumption therefore does not hold with its validity decreasing with increasing upstream Mach number. This results in a decrease in R_{uT} across the shock indicating a change in Pr_T value. In the past, variable Pr_T turbulence models have shown potential in predicting wall heat flux for SBLI flows [10].

In the current work, we study the evolution of $\overline{u'T'}$ across a shock wave. The upstream disturbance field is assumed to be purely vortical with no acoustic and entropy components. This yields $\overline{u'T'} = R_{uT} = 0$ upstream of the shock wave. Linearized transport equations for temperature fluctuations and velocity-temperature correlation are derived. The governing differential equations are integrated across the high gradient region of the shock wave and linear analysis is used to compute a budget of the source terms.

The value and sign of the downstream correlation $u'_2T'_2$ depends on the upstream Mach number (M) and the angle of incidence of the wave front (ψ). Three representative cases having $\psi = 45^\circ$, 60° and 75° are considered and the correlation just across the shock is studied for varying upstream Mach number. Superposition of the component waves for a given upstream energy spectrum yields the turbulence statistics downstream of the shock. Dominant mechanisms contributing to the generation of $\overline{u'T'}$ at the shock are thus identified. R_{uT} is calculated for varying upstream Mach numbers to highlight the limitations of Morkovin's hypothesis.

2. Flow Description

A steady, 1D, uniform mean flow is considered upstream and downstream of a normal shock. The mean flow upstream of the shock carries a purely vortical turbulence which is homogeneous and isotropic in nature. The shock is distorted from its mean position by a distance $\xi(y, z, t)$. The temporal derivative of shock deviation given by ξ_t represents the stream wise velocity of the shock wave. The transverse derivative ξ_y and ξ_z denote the angular deviation of the shock in $x - y$ and $x - z$ planes respectively. (See Fig. 1)

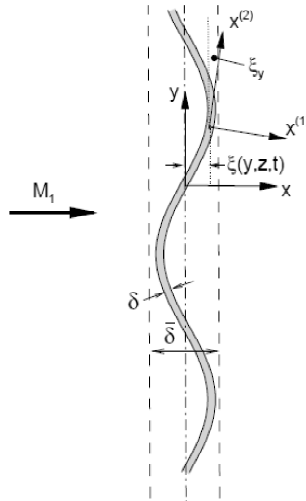


Figure 1: Schematic showing a shock wave distorted upon interaction with turbulent fluctuations [11]

In a frame of reference stationary with respect to the shock, the coordinates are given by $x^{(1)}$, $x^{(2)}$ and $x^{(3)}$ where $x^{(1)}$ represents the shock normal coordinate. $x^{(2)}$ and $x^{(3)}$ represent shock parallel coordinates. The associated velocities in these coordinates are $u^{(1)}$, $u^{(2)}$ and $u^{(3)}$ respectively. Considering small deviation of the shock from its mean location, transformation to lab frame of reference can be achieved by employing the below formulation.

$$x^{(1)} = x - \xi - y\xi_y - z\xi_z \quad (2a)$$

$$x^{(2)} = y + x\xi_y, \quad (2b)$$

$$x^{(3)} = z + x\xi_z \quad (2c)$$

$$u^{(1)} = u - \xi_t - v\xi_y - w\xi_z \approx \bar{u} + u' - \xi_t \quad (3a)$$

$$u^{(2)} = v + u\xi_y \approx \bar{u}\xi_y + v', \quad (3b)$$

$$u^{(3)} = w + u\xi_z \approx \bar{u}\xi_z + w', \quad (3c)$$

Here x , y and z represent the coordinates in lab frame of reference having corresponding velocity components u , v and w . This transformation is useful in carrying out the order of magnitude analysis as shown in next section.

3. Transport Equation for $\overline{u'T'}$

The energy conservation equation written in the frame of reference attached to the shock is given by,

$$\frac{\partial}{\partial x^{(1)}} \left(h + \frac{(u^{(1)})^2}{2} \right) = 0 \quad (4)$$

Here, h represents the enthalpy.

In the above equation, the temporal derivative and the transverse derivative have been neglected as they are small in comparison to shock-normal derivative. (For details refer [11]) Although, viscous terms are large in the high gradient shock region, they have negligible contribution to the post shock turbulence statistics and are hence dropped. Transforming Eq. (4) into lab frame of reference using Eqns. (2a-2c) and Eqns. (3a-3c) we get,

$$C_p \frac{\partial}{\partial x} (\bar{T} + T') + \frac{1}{2} \frac{\partial}{\partial x} (\bar{u} + u' - \xi_t)^2 = 0 \quad (5)$$

For the given case where fluctuations are small as compared to the mean flow, the above equation can be linearized to obtain,

$$C_p \frac{\partial T'}{\partial x} = -(u' - \xi_t) \frac{\partial \bar{u}}{\partial x} - \bar{u} \frac{\partial u'}{\partial x} \quad (6)$$

The first term on the right hand side represents the generation of temperature fluctuations due to gradient in mean velocity. When $(u' - \xi_t)$ is positive, this term has a positive contribution towards temperature fluctuations generated. The second term signifies the negative correlation between velocity and temperature fluctuation. Decrease in velocity fluctuation across the shock leads to an increase in temperature fluctuation and vice-versa. Taking a moment of Eq. 6 about u' and Reynolds averaging, we obtain,

$$C_p \frac{\partial}{\partial x} \overline{u'T'} = -\overline{u'(u' - \xi_t)} \frac{\partial \bar{u}}{\partial x} - \bar{u} \frac{\partial}{\partial x} \left(\frac{\overline{u'^2}}{2} \right) + C_p \bar{T}' \frac{\partial \bar{u}'}{\partial x} \quad (7)$$

The first term brings in the effect of shock-unsteadiness in the generation of turbulent heat flux. The second term represents the streamwise turbulent kinetic energy. An increase in this quantity will lead to a decrease in turbulent heat flux and vice-versa.

3.1 Integrated form of equation

Integrating Eq. (4) across the shock, we obtain,

$$(h_2 - h_1) + \frac{1}{2} \left[(u_2^{(1)})^2 - (u_1^{(1)})^2 \right] = 0$$

The subscript '2' refers to downstream condition and '1' refers to upstream condition. Again, the superscript (1) refers to streamwise velocity in the frame of reference stationary with respect to shock. Linearizing the above equation and rearranging we get,

$$C_p(T_2' - T_1') = -(u_m' - \xi_t)(\bar{u}_2 - \bar{u}_1) - \bar{u}_m(u_2' - u_1') \quad (8)$$

where $\bar{u}_m = (\bar{u}_1 + \bar{u}_2)/2$. The above equation is the integrated form of Eq. (6). Taking a moment of this equation about u_m' and averaging we get,

$$C_p(\overline{u_2' T_2'} - \overline{u_1' T_1'}) = -\overline{u_m'(u_m' - \xi_t)(\bar{u}_2 - \bar{u}_1)} - \bar{u}_m \frac{1}{2} [\overline{(u_2')^2} - \overline{(u_1')^2}] + C_p \overline{T_m'(u_2' - u_1')} \quad (9)$$

where $u_m' = (u_1' + u_2')/2$. The above equation is the integrated form of Eq. (9). For the case that is chosen, $T_1' = 0$. Therefore, Eq. (9) reduces to,

$$C_p \overline{u_2' T_2'} = -\overline{u_m'(u_m' - \xi_t)(\bar{u}_2 - \bar{u}_1)} - \bar{u}_m \frac{1}{2} [\overline{(u_2')^2} - \overline{(u_1')^2}] + C_p \overline{T_2'(u_2' - u_1')} \quad (10)$$

4. Budget of Turbulent heat flux

The budget of Eq. (10) is obtained using LIA, which models the upstream fluctuations as waveforms. As only vortical fluctuations are considered upstream of the shock, the velocity fluctuations are given by

$$\begin{aligned} \frac{u_1'}{\bar{u}_1} &= l A_v \exp[i\kappa(mx + ly - \bar{u}_1 mt)] \\ \frac{v_1'}{\bar{u}_1} &= -m A_v \exp[i\kappa(mx + ly - \bar{u}_1 mt)] \end{aligned}$$

where $m = \cos\psi$ and $l = \sin\psi$, ψ being the angle of incidence of the wave with the mean flow direction.

Here, A_v represents the magnitude and κ represents the wavenumber of the vortical wave. Further, the upstream turbulence is modeled as spectrum of such waves having different wavenumbers and incidence angles. LIA considers each of these waves to interact independently with the shock. The full turbulent statistics downstream of the shock is obtained by linear superposition of each of these interactions. LIA formulation can be found in work of Mahesh et al. [9]. Studying each of these waves independently helps in analyzing the full turbulence spectrum.

4.1 Single wave analysis

A single wave analysis is carried out by studying the budget of Eq. (10) for varying incidence angles of vortical wave. For this analysis, the magnitude of A_v is taken as 1. Throughout this work, the velocity variables have been normalized by the speed of sound downstream of the shock, \bar{a}_2 and the temperature variables have been normalized by \bar{a}_2^2/C_p , where C_p is the specific heat of air at constant pressure. A non-dimensional value of 1 has been taken for C_p and the value of γ is taken to be 1.4.

Incidence angle $\psi = 45^\circ$

Fig. 2 shows the budget of Eq. (10) for a point just across the shock for varying upstream Mach numbers. $\overline{u'T'}$ is zero for $M = 1$ and increases steadily for higher Mach numbers. The first term in the RHS of Eq. (10) is represented as S_1 . This term brings in effect of shock unsteadiness and has a positive contribution to $\overline{u'T'}$. The second term represented as S_2 signifies the effect of streamwise turbulent kinetic energy (TKE) change on $\overline{u'T'}$. By analyzing the budget, it can be seen that the streamwise TKE decreases across the shock which in turn has a positive contribution effect on the generation of $\overline{u'T'}$. The third term in the RHS of Eq. (10) is the correlation of the streamwise velocity difference with downstream temperature fluctuation. This term has a negative contribution to the generation of $\overline{u'T'}$.

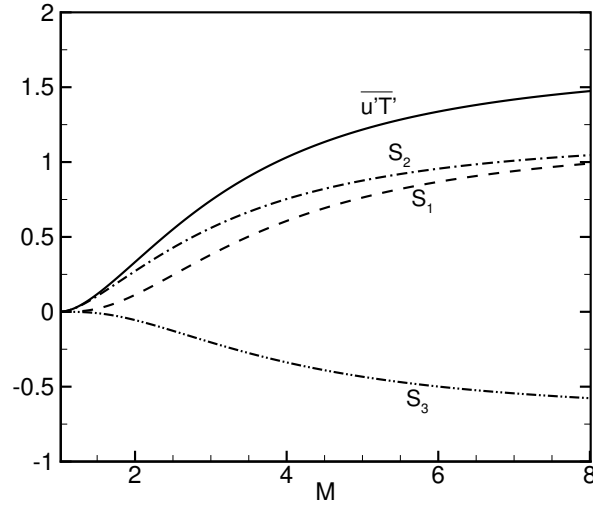


Figure 2: Budget of Eq.(10) computed for a 2D plane wave at $\psi = 45^\circ$ interacting with a normal shock of varying strength

Incidence angle $\psi = 60^\circ$

The budget for Eq. (10) for varying upstream Mach numbers can be found in Fig. 3. As seen in the figure, $\overline{u'T'}$ has negative value at low Mach numbers and takes positive values as Mach number increases. The point where $\overline{u'T'} = 0$ (corresponding to $M = 2.25$) is of interest. At this point, shock is moving with a speed ξ_t equivalent to the upstream streamwise velocity fluctuation i.e. $\xi_t = u'_1$. The flow passes through the shock without experiencing the effect of shock distortion i.e. $u'_1 = u'_2$. Also, for this particular Mach number, there is no generation of acoustic and entropy modes downstream resulting in $p'_2 = T'_2 = \rho'_2 = 0$. In the low Mach number region, $\overline{u'T'}$ closely follows the term S_2 which represents the change in TKE across the shock. As seen in the 45° case, both S_1 and S_2 have positive contribution to generation of $\overline{u'T'}$ at higher Mach numbers whereas S_3 has a negative contribution both at higher and lower Mach numbers.

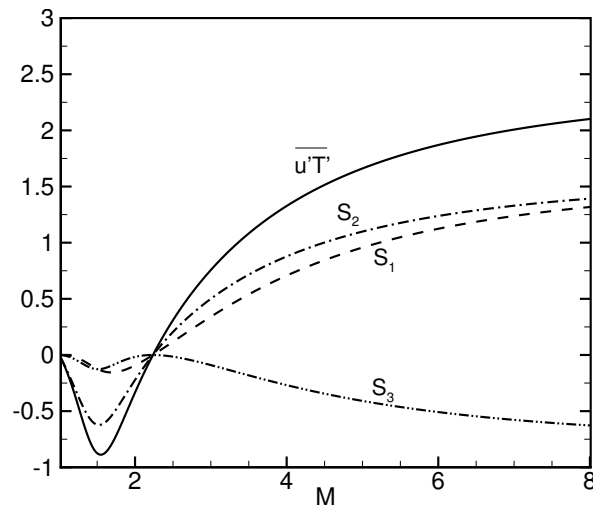


Figure 3: Budget of Eq.(10) computed for a 2D plane wave at $\psi = 60^\circ$ interacting with a normal shock of varying strength

Incidence angle $\psi = 75^\circ$

Fig. 4 shows budget of Eq. (10) for varying upstream Mach numbers. $\overline{u'T'}$ has a sharp dip at a low Mach number ($M = 1.04$) and remains negative for a large range of Mach numbers. This dip can be attributed to the fact that $\psi = 75^\circ$ represents the critical angle for $M = 1.04$. At this Mach number, the nature of acoustic wave downstream of the shock changes from propagating to decaying. Single waves corresponding to this angle with Mach number $M > 1.04$ will yield decaying acoustic fluctuations downstream of the shock. Both S_1 and S_2 terms have positive contribution to the generation of $\overline{u'T'}$, which are over weighed by negative contribution from the term S_3 .

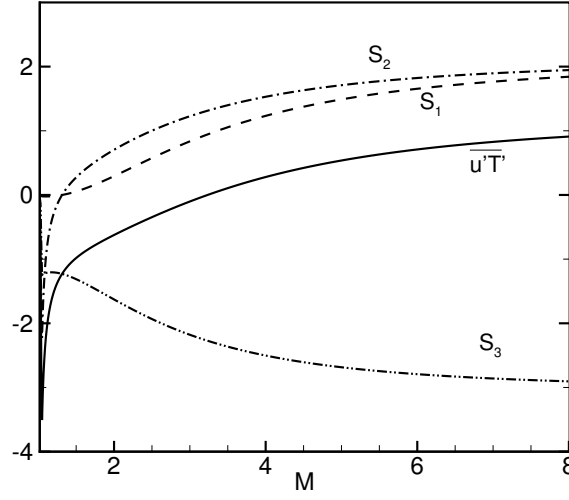


Figure 4: Budget of Eq.(10) computed for a 2D plane wave at $\psi = 75^\circ$ interacting with a normal shock of varying strength

4.2 Three-dimensional spectrum

The upstream turbulence is modeled as a spectrum of waves having an energy distribution given by

$$E(k) \sim \left(\frac{k}{k_o}\right)^4 e^{-2\left(\frac{k}{k_o}\right)^2}$$

where, k_o corresponds to wavenumber having peak energy.

The turbulent statistics downstream is obtained by integrating results obtained over all wavenumbers and inclination of upstream wave angles. For example,

$$\left(\overline{u'_2 T'_2}\right)_{3D} = 4\pi \int_{k=0}^{\infty} \int_{\psi_1=0}^{\frac{\pi}{2}} \left(\overline{u'_2 T'_2}\right)_{2D} k^2 \sin \psi_1 d\psi_1 dk$$

where, $\left(\overline{u'_2 T'_2}\right)_{2D}$ represents result for a 2D planar wave.

The near-field budget of Eq. (10) for a purely vortical turbulence is plotted in Fig. 5 for varying upstream Mach number. At low Mach numbers, the value of $\overline{u'T'}$ remains negative and rises to a positive value for higher Mach numbers. This trend was observed in single wave analysis when $\psi = 60^\circ$ and 75° .

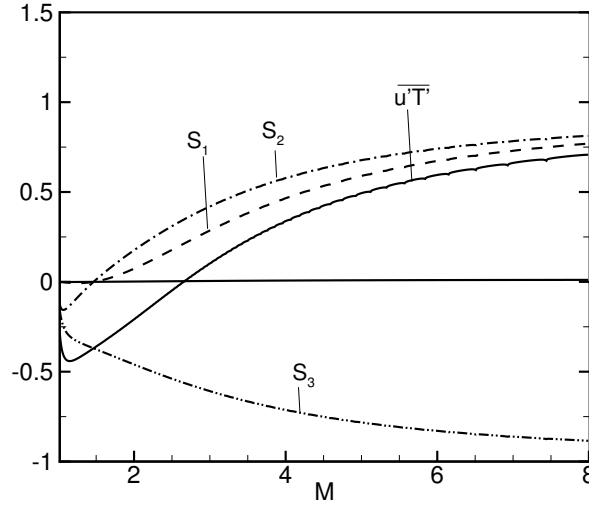


Figure 5: Budget of Eq.(10) computed for a 3D spectrum of waves interacting with a normal shock of varying strength

R_{uT} Analysis

In turbulent boundary layers, R_{uT} is close to -1 indicating the negative correlation between velocity and temperature fluctuation. Conventional modeling of turbulent heat flux vector $\rho u'T'$ in the energy conservation equation relies on this assumption of negative correlation. Fig. 6 shows the value of near-field R_{uT} for varying upstream Mach numbers for three-dimensional turbulence under consideration. The trend closely follows the value of $\overline{u'T'}$ for the range of Mach numbers as seen in the figure. As can be seen, R_{uT} takes both negative and positive values depending on upstream Mach number. Therefore, it is essential to re-model turbulent heat flux vector based on this non-monotonic variation of R_{uT} .

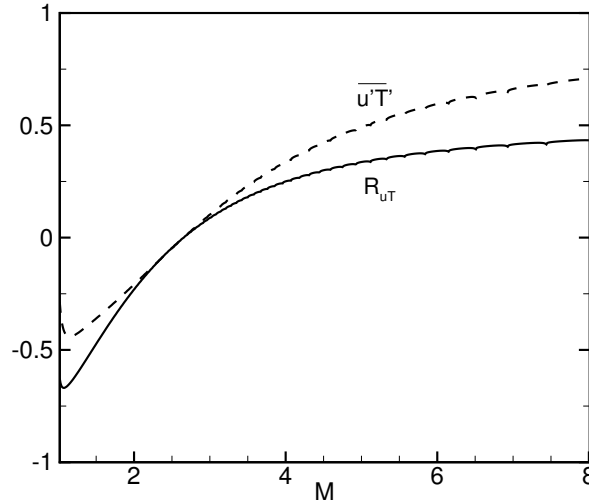


Figure 6: R_{uT} value across the shock for varying upstream Mach number

5. Conclusion

This paper studies the generation of turbulent heat flux $\overline{u'T'}$ when a homogeneous isotropic turbulence comprising of purely vortical disturbances interacts with a normal shock. A linearized energy conservation equation in a frame of reference stationary with respect to the unsteady shock wave is derived which is used to obtain an equation for the generation of $\overline{u'T'}$ across the shock. An integrated form of the equation is used to compute a budget of the heat flux

across the shock, using results from linear interaction analysis. It is found that in the 3D interaction, $\overline{u'T'}$ changes sign from negative values at lower upstream Mach numbers to positive values at higher Mach numbers. The trends are similar to that observed in case of 2D component waves at 60 and 75 deg angles of incidence. The correlation coefficient for the velocity and temperature fluctuations is studied as a function of shock strength. A clear violation from Morkovin's hypothesis is observed behind the shock wave.

References

- [1] Thivet, F., Knight, D. D., Zheltovodov, A. A., and Maksimov, A. I. 2001. Importance of limiting the turbulent stresses to predict 3D shock-wave/boundary-layer interactions. In: *23rd International Symposium on Shock Waves, Fort Worth, TX*. 2761.
- [2] Durbin, P. A. 1996. On the $k - \epsilon$ stagnation point anomaly. *Int. J. Heat Fluid Flow*. 17:89
- [3] Shih, T. H., Liou, W. W., Shabbir, A., Yang, Z. and Zhu, J. 1995. A new $k - \epsilon$ eddy viscosity model for high Reynolds number turbulent flows. *Comput. Fluids*. 24:227
- [4] Sinha, K., Mahesh, K., and Candler, G. V. 2003. Modeling shock-unsteadiness in shock/turbulence interaction. *Physics of Fluids*. 15:2290
- [5] Pasha, A. A. and Sinha, K. 2012. Shock-unsteadiness model applied to hypersonic shock-wave/turbulent boundary-layer interactions. *Journal of Propulsion and Power*. 28:46
- [6] Sinha, K., Mahesh, K., and Candler, G.V. 2005. Modeling the effect of shock unsteadiness in shock-wave / turbulent boundary layer interactions. *AIAA Journal*. 43:586
- [7] Pasha, A. A. and Sinha, K. 2008. Shock-unsteadiness model applied to oblique shock-wave/turbulent boundary layer interaction. *Int. J. Comput. Fluid Dyn.*. 22:569-582.
- [8] Morkovin, M. V. 1961. Effects of compressibility on turbulent flows. In: *Mecanique de la Turbulence (ed. A. Favré), Editions du Centre National de la Recherche Scientifique. Paris*. 367–380
- [9] Mahesh, K., Lele, S. K. and Moin, P. 1997. The influence of entropy fluctuations on the interaction of turbulence with a shock wave. *Journal of Fluid Mechanics*. 334:353
- [10] Xiao, X. and Hassan, H. A. 2007. Modeling scramjet flows with variable turbulent Prandtl and Schmidt numbers. *AIAA Journal*. 45:1415
- [11] Sinha, K. 2012. Evolution of enstrophy in shock/homogeneous turbulence interaction. *Journal of Fluid Mechanics*. 707:74-110